SIViP
DOI 10.1007/s11760-010-0189-1

ORIGINAL PAPER

Directional switching median filter using boundary discriminative noise detection by elimination

A. Nasimudeen · Madhu S. Nair · Rao Tatavarti

Received: 1 December 2009 / Revised: 9 September 2010 / Accepted: 6 October 2010

Abstract We propose an accurate and efficient noise detection algorithm for impulse noise removal, called the boundary discriminative noise detection by elimination (BDNDE), which retains the good characteristics of the BDND filter proposed by Ng and Ma (in IEEE Trans. Image Process. 15(6):1506–1516, 2006) while suppressing noise effectively. In order to determine whether a pixel is corrupted, the algorithm first sets the minimum and maximum boundary (threshold) values based on the localized window centered on the pixel. The thresholding helps in achieving low false-alarm and miss-detection rate (even in random noise), even up to 90% noise densities. Extensive simulation results, conducted on gray scale images under a wide range (from 10 to 90%) of noise corruption, clearly demonstrate that our enhanced switching median filter gives better results compared to existing BDND median-based filters, in terms of suppressing impulse noise while preserving image details. The proposed method is algorithmically simple and faster, compared to existing BDND, and more suitable for real-time implementation and application. The new method has shown superior performance in terms of subjective quality in the filtered image as well as objective quality in the peak signal-to-noise ratio (PSNR) measurement to that of the BDND filter.

Keywords Image denoising · Impulse noise detection · Nonlinear filter · Switching median filter

A. Nasimudeen · M. S. Nair
Department of Computer Science, Rajagiri College of Social Sciences, Kalamassery, Kochi 683104, Kerala, India
e-mail: mailto_nasim@yahoo.com

M. S. Nair (✉)
Department of Computer Science, University of Kerala, Kariavattom, Thiruvananthapuram 695581, Kerala, India
e-mail: madhu_s_nair2001@yahoo.com

R. Tatavarti
Department of Civil Engineering, Gayatri Vidya Parishad College of Engineering, Madhurawada, Visakhapatnam 530048, Andhra Pradesh, India
e-mail: rtatavarti@gmail.com

1 Introduction

Digital image could be contaminated by impulse noise during image acquisition or transmission. Two common types of impulse noise are the salt-and-pepper noise and the random-valued noise. For images corrupted by salt-and-pepper noise, the noisy pixels can take only the maximum and the minimum values in the dynamic range, thrust upon by the thresholding process, which may degrade the image quality and cause loss of details. Various methods have been proposed for the restoration of images corrupted by impulse noise. It is well known that the simple linear filters can produce serious image blurring even in the presence of low noise density.

Nonlinear filters were widely exploited due to their much improved filtering performance, in terms of impulse noise attenuation [1,2], wherein the median filter replaces the central value of an M-by-N neighborhood with its median value. One of the most popular and robust nonlinear filters is the standard median (SM) filter [3], which exploits the rank-order information of pixel intensities within a filtering window and replaces the center pixel with the median value. Due to its effectiveness in noise suppression and simplicity in implementation, various modifications of the SM filter have been introduced, such as the weighted median (WM) [4] filter and the center weighted median (CWM) [5] filter.

Published online: 26 October 2010

Conventional median filtering approaches apply the median operation to each pixel unconditionally, that is, without considering whether it is uncorrupted or corrupted. As a result, the image details contributed from the uncorrupted pixels are still subject to be filtered, and this causes image quality degradation [6,7]. An intuitive solution to overcome this problem is to implement an impulse-noise detection mechanism prior to filtering; hence, only those pixels identified as "corrupted" would undergo the filtering process, while those identified as "uncorrupted" would remain intact. By incorporating such noise detection mechanism or "intelligence" into the median filtering framework, the so-called switching median filters [8–15] had shown significant performance improvement.

The earlier developed switching median filters were commonly found, being nonadaptive to a given, but unknown, noise density and prone to yielding pixel misclassifications especially at higher noise density interference. To address the pixel misclassification issue in switching median filters at high noise density, the noise adaptive soft-switching median (NASM) filter was proposed in [13], which consists of a three-level hierarchical soft-switching noise detection process. The NASM achieves a fairly robust performance in removing impulse noise, while preserving signal details across a wide range of noise densities. However, the quality of the recovered image becomes significantly degraded when noise density is greater than 50%. To overcome the pixel misclassification and performance degradation at high noise density (i.e., >50%), a new efficient method called BDND [16] was demonstrated to yield better results. However, it was found that the BDND filter showed higher misdetection and false-alarm rate at very high noise densities (>80%), which in turn demonstrated a significant reduction in the image quality in addition to nonpreservation of the edge details of the image. Subsequently, a modified switching median filter based on BDND [17] was proposed, which showed only marginal improvement over BDND.

In this paper, we introduce an easy method for impulse noise detection, which not only yields significant improvement on the existing BDND filter, but also drastically minimizes the problems of misdetection and false-alarm rate even for images with very high noise density (90%). The proposed technique significantly improves the noise filtering characteristics by applying a new directional filtering process, conditionally across the filtering window, leading to the preservation of edge details. Consequently, the proposed image restoration method is simple, accurate and faster compared to the existing BDND switching median filters.

In the following sections, we introduce the proposed detection algorithm for impulse noise identification (Sect. 2), the filtering scheme in response to the noise detection results (Sect. 3) and extensive simulation results (Sect. 4).

2 Impulse noise detection method

2.1 Noise models

A set of four standard impulse noise models [16] are implemented for extensively examining the performance of the proposed filter considering practical situations, as follows.

Noise Model 1: Noise is modeled as salt-and-pepper impulse noise as practiced, for example, in [11]. Noise is modeled as salt-and-pepper impulse noise, pixels are randomly corrupted by two fixed extreme values, 0 and 255 (for 8-bit monochrome image), generated with the same probability. That is, for each image pixel at location (i, j) with intensity value S_{ij}, the corresponding pixel of the noisy image will be x_{ij}, in which the probability density function of x_{ij} is

$$f(x) = \begin{cases} \frac{p}{2}, & \text{for } x = 0 \\ 1-p, & \text{for } x = S_{ij} \\ \frac{p}{2}, & \text{for } x = 255 \end{cases}, \; p \text{ is the noise density.}$$

Noise Model 2: Model 2 is similar to Model 1, except that each pixel might be corrupted by either "pepper" noise (i.e., 0) or "salt" noise with unequal probabilities. That is,

$$f(x) = \begin{cases} p1, & \text{for } x = 0 \\ 1-p, & \text{for } x = S_{ij} \\ p^2, & \text{for } x = 255 \end{cases}$$
$$p = p1 + p2 \quad \text{is the noise density and} \, p1 \neq p2.$$

Noise Model 3: Instead of two fixed values, impulse noise could be more realistically modeled by two fixed ranges that appear at both ends with a length of m each, respectively. For example, if m is 10, noise will equal likely be any values in the range of either [0, 9] or [246, 255] . That is,

$$f(x) = \begin{cases} \frac{p}{2m}, & \text{for } 0 \leq x < m \\ 1-p, & \text{for } x = S_{ij} \\ \frac{p2}{m}, & \text{for } 255 - m < x \leq 255 \end{cases},$$
$$p \quad \text{is the noise density.}$$

Noise Model 4: Model 4 is similar to Model 3, except that the densities of low-intensity impulse noise and high-intensity impulse noise are unequal. That is,

$$f(x) = \begin{cases} \frac{p1}{m}, & \text{for } 0 \leq x < m \\ 1-p, & \text{for } x = S_{ij} \\ \frac{p2}{m}, & \text{for } 255 - m < x \leq 255 \end{cases},$$
$$p = p1 + p2 \quad \text{is the noise density and} \, p1 \neq p2.$$

2.2 Existing boundary discriminative noise detection (BDND)

The existing BDND [16] algorithm is applied to each pixel of the noisy image in order to identify whether it is 'uncorrupted' or 'corrupted'. After such an application to the entire

image, a two-dimensional binary decision map is formed at the end of the noise detection stage, with '0s' indicating the positions of 'uncorrupted' pixels and '1s' for those of 'corrupted' ones.

To accomplish this objective, all the pixels within a predefined window that center on the considered pixel will be grouped into three clusters; hence, two boundaries are required to be determined. For each pixel x_{ij} being considered, if $0 \leq x_{ij} \leq b1$, the pixel will be assigned to the lower-intensity cluster, to the medium-intensity cluster for $b1 \leq x_{ij} \leq b2$, otherwise to the high-intensity cluster for $b2 \leq x_{ij} \leq 255$. If the center pixel being considered falls onto the middle cluster, it will be treated as 'uncorrupted', since its intensity value is neither relatively low nor relatively high. Otherwise, it is very likely that the pixel has been corrupted by impulse noise. Clearly, the accuracy of clustering results (hence, the accuracy of noise detection) ultimately depends on how accurate the identified boundaries $b1$ and $b2$ are.

The boundary discriminative process consists of two iterations, in which the second iteration will be invoked conditionally. In the first iteration, an enlarged local window with a size of 21×21 is used to examine whether the considered pixel is an uncorrupted one. If the pixel fails to meet the condition to be classified as uncorrupted (i.e., not falling onto the middle cluster), the second iteration will be invoked to further examine the pixel based on a more confined local statistic, by using a 3×3 window [4].

2.3 Boundary Discriminative Noise Detection by Elimination (BDNDE)

As in the case of BDND, the proposed algorithm is applied to each pixel of a noisy image in order to identify whether the pixel is 'corrupted' or 'uncorrupted'. A two-dimensional binary decision map is formed at the end of the detection phase, with '0' indicating the position of uncorrupted pixels and '1' indicating the position of corrupted ones. To accomplish this, the algorithm replaces the high intensity and low-intensity pixels from the list with the minimum and maximum boundary values from the remaining intensity values. If the considered pixel is within the boundary region defined by the two boundary values, then it will be classified as 'uncorrupted', otherwise it is construed that the pixel has been 'corrupted' by impulse noise. Hence, two boundaries $b1$ and $b2$ are required to be determined for each pixel being considered.

All the pixels within a pre-defined window centered on a pixel being considered will be sorted, and then all the minimum and maximum intensity values from the sorted list will be removed. From the reduced list, we will get the second minimum and maximum, and these values will be set as the boundary values $b1$ and $b2$. If there is no value in the remaining list after elimination, the minimum and maximum will be taken as $b1$ and $b2$. So for, each pixel x_{ij} being considered, if $b1 \leq x_{ij} \leq b2$, then the pixel would be treated as 'uncorrupted'.

Table 1 Suggested window size for the estimated noise density level p

Noise density	$W_{D1} \times W_D1$
$0\% < p \leq 20\%$	3×3
$20\% < p \leq 40\%$	5×5
>40%	7×7

The proposed process consists of two iterations, in which the second iteration will be invoked conditionally. In the first iteration, an enlarged local window with a size of 21×21 (empirically determined) is used to examine whether the considered pixel is an uncorrupted one. If the pixel is uncorrupted, then the second iteration will be invoked to further examine the pixel based on a more confined local statistics by using a 5×5 window, to make sure that the pixel is uncorrupted. In summary, the steps of the proposed detection method are as follows:

Step (1) *Impose a* 21×21 *window, which is centered on the current pixel.*

Step (2) *Sort the pixels in the window in ascending order of intensity values and find minimum and maximum values.*

Step (3) *Remove the items with minimum and maximum intensity values.*

Step (4) *If the remaining list contains no value, then the minimum and maximum will be set as b1 and b2, otherwise b1 and b2 will be the new minimum and maximum from the reduced list.*

Step (5) *If the pixel not belongs to the range defined by b1 and b2, it is classified as 'corrupted' pixel, and the classification process stops for this pixel; else, the second iteration will be invoked in the following.*

Step (6) *Impose a* 5×5 *window, being centered on the concerned pixel and repeat Steps* 2–5.

Step (7) *If the pixel under consideration belongs to the cluster defined by boundaries, it is classified as 'uncorrupted' pixel, otherwise 'corrupted'.*

For the understanding of the algorithmic steps mentioned above, a 5×5 windowed subimage (instead of 21×21) with the center pixel "165" is used as an example for illustrating the proposed detection process as follows:

$$W = \begin{pmatrix} 255 & 0 & 47 & 255 & 42 \\ 255 & 50 & 255 & 0 & 0 \\ 0 & 0 & 165 & 198 & 205 \\ 55 & 255 & 0 & 0 & 255 \\ 255 & 65 & 49 & 0 & 204 \end{pmatrix}.$$

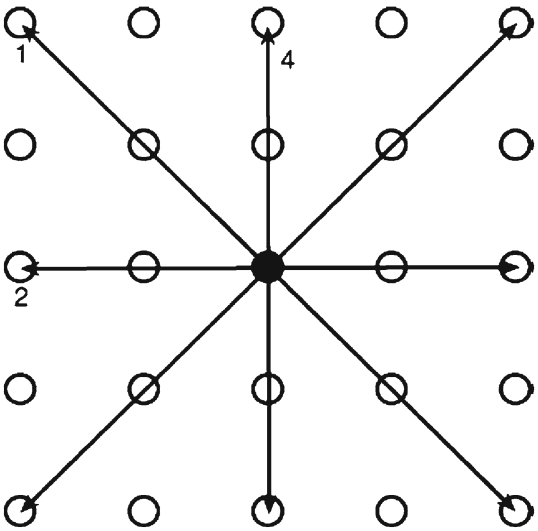

Fig. 1 An example of four directions for filtering window of size 5

- Pixel intensities are sorted in the ascending order and represented as a vector, i.e., V = [0 0 0 0 0 0 0 0 42 47 49 50 55 65 165 198 204 205 255 255 255 255 255 255 255 255]. Here, the minimum and maximum values are 0 and 255, respectively.
- Remove the minimum and maximum intensity values from the vector V. Thus, the reduced vector V = [42 47 49 50 55 65 165 198 204 205]. Since the list is nonempty, the boundary values will be the new minimum and maximum; here, it will be $b1$=42 and $b2$=205. If the list is empty after the elimination, then the maximum and minimum (i.e., 0 and 255) will be considered as the boundaries $b1$ and $b2$.
- Since the center pixel '165' belongs to the range defined by $b1$ and $b2$, second iteration will be invoked with a closer window (5×5) to confirm that it is uncorrupted. If the pixel is not within the range, then it is classified as corrupted, and no further iteration is needed.

Fig. 2 First columns shows three original test images: (*top*) "Lena," (*middle*) "Cameraman," and (*bottom*) "Tire," and the second column presents their corresponding noisy images with 80% impulse noise corruption generated by Noise Model 1

3 Improved switching median filter

3.1 Noise density estimation

The size of the filtering window is determined using the same procedure described in the BDND filter. Initially, the limit of the maximum window size requires being determined. Accordingly, Table 1 is empirically established based on multiple test images, in which different window sizes are suggested for different noise density levels. The noise density can be estimated simply by counting the number of 1s in the binary decision map obtained from the impulse noise detection stage. Based on the binary decision map, 'no filtering' is applied to those 'uncorrupted' pixels, while the enhanced switching median filter with an adaptively determined window size is applied to each 'corrupted' one.

3.2 Existing noise adaptive filtering

In the filtering, the maximum size of the filtering window is determined based on the percentage of noise. The size of the filtering window starts with 3 and iteratively extends outward by one pixel in all the four sides of the window, provided that the number of uncorrupted pixels is less than the total number of pixels within the filtering window and at the same time, the window size should be less than the maximum. An additional condition is established that the window will also be extended when the number of uncorrupted pixels is equal to zero. Then, the switching median filter is applied on the filtering window, i.e., only those 'uncorrupted' pixels within the window are considered for the process of ranking.

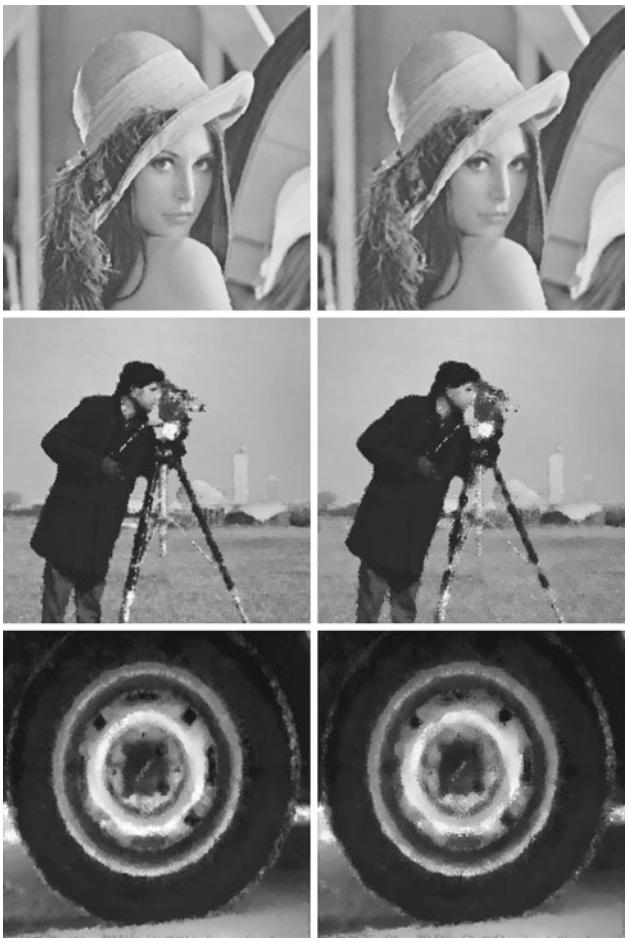

Fig. 3 Results of denoising corrupted images "Lena," "Cameraman," and "Tire" (with 80% impulse noise density (model1)) by using proposed directional switching median filter (*first column*), the existing switching median filter with the BDND incorporated (*second column*), respectively

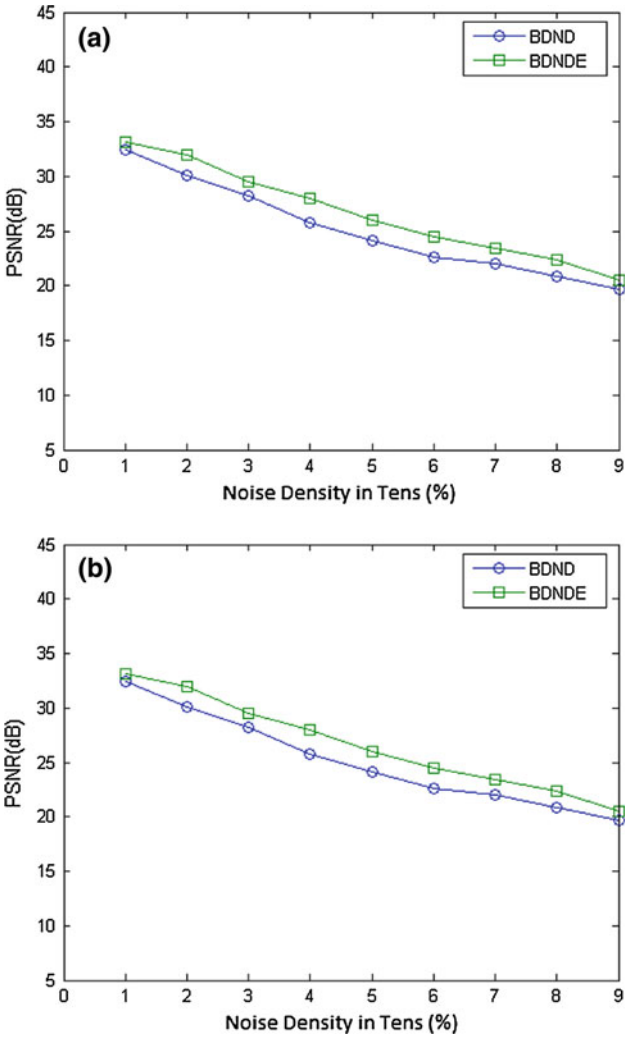

Fig. 4 PSNR performance comparison of using the BDND, the proposed directional switching median filter on: **a** "Cameraman;" and **b** "Lena;" corrupted by various noise densities

3.3 Enhanced noise adaptive filtering

After impulse detection, BDND-based switching median filter replace the noisy pixels by median values of true pixels in the window. Here, we will improve the outputs of filter based on the information of the four directions. Compared to the BDND's filtering stage, there are two changes for further performance improvement. Once the maximum filtering window size is determined (W_{D1}), as in the case of BDND, the filtering window start with size 3 ($W_F = 3$). But the filtering window iteratively extends outward by two pixel in all the four sides of the window (needed for directional filtering), provided that the number of uncorrupted pixels (denoted by N_c) is less than half of the total number of pixels (denoted by $S_{\text{in}} = (1/2)[W_F \times W_F]$) within the filtering window, while $W_F \leq W_{D1}$, and the filtering window can also be extended when the number of uncorrupted pixels is equal to zero. Thus, the condition for extending window is $while\ (N_{1c} < S_{1\text{in}}\ and\ W_{1F} \leq W_{1D1})$ or $N_{1c} = 0$.

In BDND, the filtering is applied by taking the median value of the entire filtering window. In our proposed method, performance is improved by applying the condition of directionality on the filtering window W, where

$$W = \left\{(s,t)| - \frac{W_F - 1}{2} \leq s,t \leq \frac{W_F - 1}{2}\right\}$$

The proposed method focuses on the four main directions and utilizes a 3×3 closer window for filtering, as shown in Fig. 1. Only uncorrupted pixels within the window W will be considered. Let D_K (K=1 to 5) denote a set of coordinates aligned with the direction centered at (0, 0) on the filtering

Table 2 PSNR performance, Miss Detection (MD), False Alarm (FA) and Execution Time (*secs*) resulted after applying the BDND and the new method individually applied to noisy (noise model 1 with two iterations) images (a) "Tire," (b) "Cameraman,"(c) "Pout," and (d) "Aerial," corrupted under various noise densities

Noise %	PSNR (BDND)	PSNR (New)	MD (BDND)	MD (New)	FA (BDND)	FA (New)	Time (BDND)	Time (New)
(a) Image 'Tire'								
30	30.48	32.31	0	0	917	739	9.734	6.219
50	25.86	28.08	0	0	788	584	10.265	6.937
70	23.38	25.43	0	0	746	508	11.187	7.719
90	20.71	21.34	0	0	692	434	11.594	8.187
(b) Image 'Cameraman'								
30	27.72	29.30	0	0	234	146	13.047	8.515
50	24.25	26.02	0	0	222	5	14.109	9.578
70	22.03	23.34	0	0	207	0	15.266	10.672
90	19.74	20.38	0	0	192	0	15.953	11.282
(c) Image 'Pout'								
30	42.47	43.07	0	0	0	123	12.922	8.547
50	37.22	38.50	0	0	0	7	13.875	9.516
70	33.64	35.10	0	0	3	1	15.219	10.703
90	30.83	31.29	0	0	30	0	15.954	11.282
(d) Image 'Aerial'								
30	29.80	30.43	0	0	304	275	13.329	8.563
50	25.98	27.07	0	0	240	189	14.265	9.547
70	22.97	24.36	0	0	219	169	15.360	10.719
90	20.77	21.33	0	0	206	116	16.031	11.313

Table 3 PSNR performance, MD, FA and Execution Time (*secs*) resulted after applying the BDND and the new method individually to noisy (noise model 2) images (a) "Tire," (b) "Cameraman,"(c) "Pout," and (d) "Aerial," corrupted under various noise densities

Noise %	PSNR (BDND)	PSNR (New)	MD (BDND)	MD (New)	FA (BDND)	FA (New)	Time (BDND)	Time (New)
(a) Image 'Tire'								
30	29.80	32.11	0	0	920	638	9.641	5.219
50	25.93	28.15	0	0	829	589	10.219	6.203
70	23.44	25.55	0	0	711	502	11.062	7.312
90	20.60	21.60	0	0	717	435	11.578	8.047
(b) Image 'Cameraman'								
30	27.98	29.68	0	0	232	0	14.156	7.781
50	23.98	25.80	0	0	229	0	14.157	8.609
70	21.90	23.27	0	0	199	0	15.234	10.109
90	19.58	20.32	0	0	189	0	15.953	11.109
(c) Image 'Pout'								
30	42.97	43.29	0	0	0	0	12.937	7.157
50	37.43	38.85	0	0	0	0	13.907	8.594
70	33.73	35.19	0	0	2	0	15.156	10.109
90	30.83	31.43	0	0	69	0	15.907	11.125
(d) Image 'Aerial'								
30	29.99	30.65	0	0	322	211	13.312	7.140
50	26.16	27.25	0	0	255	186	14.078	8.625
70	23.01	24.33	0	0	209	160	15.297	10.125
90	20.85	21.28	0	0	276	142	15.985	11.109

Fig. 5 Results of denoising corrupted images "Lena," "Cameraman," and "Tire" (with 50% impulse noise density(30% salt and 20% pepper)) by using proposed directional switching median filter (*first column*), the existing switching median filter with the BDND incorporated (*second column*), respectively

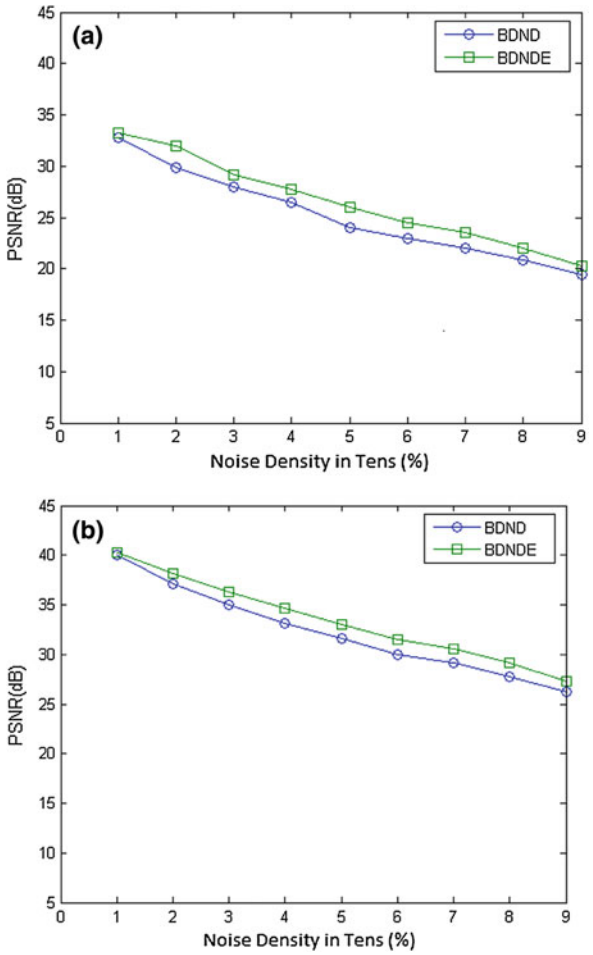

Fig. 6 PSNR performance comparison of using the BDND, the proposed directional switching median filter on: **a** "Cameraman;" and **b** "Lena;" corrupted by various noise densities (model2)

Table 4 PSNR performance, MD, FA and Execution Time (*secs*) resulted after applying the BDND and the new method individually to noisy (noise model 3) images (a) "Tire," (b) "Cameraman,"(c) "Pout," and (d) "Aerial," corrupted under various noise densities

Noise %	PSNR (BDND)	PSNR (New)	MD (BDND)	MD (New)	FA (BDND)	FA (New)	Time (BDND)	Time (New)
(a) Image 'Lena'								
30	25.24	28.36	4,824	4,620	1,629	2,310	9.42	6.23
50	24.80	27.23	6,594	5,806	1,696	1,734	9.80	6.78
70	23.34	24.32	6,243	5,440	969	1,067	10.58	7.70
(b) Image 'Cameraman'								
30	26.47	29.44	3	21	795	164	13.09	8.53
50	24.31	25.71	0	0	225	11	14.02	9.53
70	22.00	23.50	0	0	235	0	15.27	10.69
(c) Image 'Pout'								
30	42.53	43.05	0	0	0	108	12.92	8.53
50	37.38	38.53	0	0	0	10	13.95	9.58
70	33.89	35.59	0	0	12	1	15.25	10.75
(d) Image 'Aerial'								
30	28.69	30.39	179	235	495	287	13.36	8.64
50	25.01	26.89	252	281	309	148	14.17	9.58
70	23.22	24.40	75	191	124	66	15.27	10.70

Fig. 7 Results of denoising corrupted images "Lena," "Cameraman," and "Tire" (with 50% impulse noise density(30% salt and 20% pepper)) by using proposed directional switching median filter (*first column*), the existing switching median filter with the BDND incorporated (*second column*) respectively

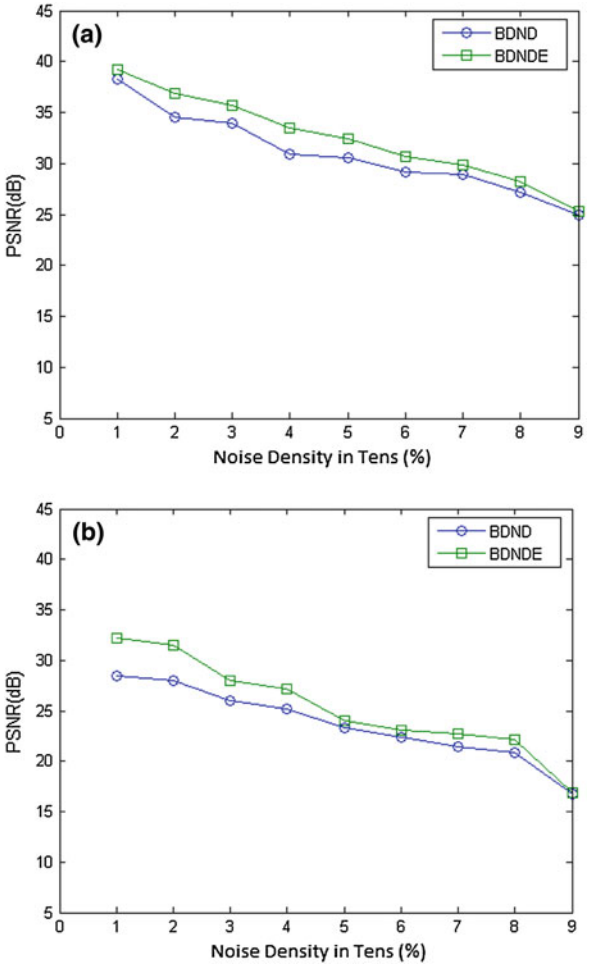

Fig. 8 PSNR performance comparison of using the BDND, the proposed directional switching median filter on: **a** "Cameraman;" and **b** "Lena;" corrupted by various noise densities (model3)

window ($W_F \times W_F$) i.e.,

$$D_1 = \{(-y,-y),\ldots,(-1,-1),(0,0),(1,1),\ldots,(y,y)\}$$
$$D_2 = \{(0,-y),\ldots,(0,-1),(0,0),(0,1),\ldots,(0,y)\}$$
$$D_3 = \{(y,-y),\ldots,(1,-1),(0,0),(-1,1),\ldots,(-y,y)\}$$
$$D_4 = \{(-y,0),\ldots,(-1,0),(0,0),(1,0),\ldots,(y,0)\}$$

where $y = W_F/2$. Thus, we have the new list of all uncorrupted pixels,

$$L_{i,j} = \bigcup_{k=1}^{5} D_k$$

If the number of pixels within the list ($L_{i,j}$) is less than 5 (does not have adequate information for taking median value), then the whole filtering window should be taken (uncorrupted pixels within the window) for finding median value. Let $\grave{b}$e the number of pixels in $L_{i,j}$, then the output pixel $Y_{i,j}$ is

$$Y_{1(i,j)} = \{\text{median}(L_{1(i,j))}\}, n \geq 5$$
$$= \{\text{median}(X_{1(i-s,j-t)})|(s,t)\,\epsilon W\}, n < 5$$

Thus, the proposed method can preserve more edge details when compared to BDND filter even at higher noise density.

4 Results and discussion

The performance of the proposed algorithm was evaluated based on each noise model described in Sect. 2.1. Restoration results are quantitatively measured by peak signal-to-noise ratio (PSNR). PSNR is most easily defined via the mean squared error (MSE) defined as:

$$MSE = \frac{1}{MN}\sum_{i=1}^{M}\sum_{j=1}^{N}\left(Y_{ij} - S_{ij}\right)^2$$

Table 5 PSNR performance, MD, FA and Execution Time (*secs*) resulted after applying the BDND and the new method individually to noisy (noise model 4) images (a) "Tire," (b) "Cameraman,"(c) "Pout," and (d) "Aerial," corrupted under various noise densities

Noise %		PSNR (BDND)	PSNR (New)	MD (BDND)	MD (New)	FA (BDND)	FA (New)	Time (BDND)	Time (New)
S	*P*								
(a) Image 'Lena'									
10	20	28.89	30.69	1,866	1,617	1,449	1,582	9.61	6.34
20	10	26.75	30.15	4,531	3,352	1,113	1,774	9.38	6.31
20	30	24.42	26.13	5,791	6,211	4,543	2,048	10.30	6.73
30	20	22.54	26.65	9,350	7,896	2,135	1,929	9.67	6.66
20	40	22.59	25.71	2,501	2,030	1,813	724	10.66	7.45
40	20	19.90	25.46	13,135	10,000	1,921	1,692	9.63	6.97
(b) Image 'Cameraman'									
10	20	26.64	29.14	8	32	525	289	13.11	8.58
20	10	26.46	29.17	12	64	760	284	13.16	8.56
20	30	23.87	25.78	2	8	438	21	14.14	9.53
30	20	24.01	25.91	0	0	295	10	14.05	9.53
20	40	21.42	23.74	1,611	1,428	1,678	591	14.70	10.25
40	20	22.77	24.56	7	35	260	24	14.66	10.22
(c) Image 'Pout'									
10	20	41.97	42.45	0	0	2	237	13.03	8.64
20	10	42.47	42.86	0	0	0	268	13.06	8.64
20	30	37.21	38.45	0	0	2	14	13.94	9.48
30	20	36.66	38.58	0	0	11	12	13.95	9.52
20	40	35.31	36.84	0	0	9	13	14.55	10.19
40	20	35.38	36.93	0	0	1	21	14.64	10.27
(d) Image 'Aerial'									
10	20	29.72	30.39	105	176	413	372	13.38	8.59
20	10	29.12	30.28	131	136	441	317	13.30	8.55
20	30	25.04	26.84	394	411	371	151	14.13	9.58
30	20	25.03	26.83	245	257	361	157	14.11	9.53
20	40	24.25	25.52	283	292	151	116	14.70	10.19
40	20	23.55	25.53	242	272	413	143	14.78	10.22

Where, Y and S are two $M \times N$ monochrome images. Y is considered as the original image and S is considered as the restored image. M and N are the total number of pixels in the horizontal and the vertical dimensions of the original and restored image. A higher PSNR value indicates higher image quality. The performance evaluation of the filtering operation was quantified by the PSNR, which is computed as follows:

$$PSNR = 10 \log_{10} \left(\frac{255}{MSE} \right) dB$$

Filtering of images corrupted by Noise Model 1: Although extensive simulations were carried out using several monochrome images, only images of 'Lena', 'Tire' and 'Cameraman' are chosen for demonstrations. Original images (left column) and their corrupted versions with 80% noise density (model 1) (right column) are shown side by side in Fig. 2. The filtering performance of the ideal switching filter, BDND filter and the proposed filter are shown in Fig. 3 for comparison. Fig. 4 graphically illustrates the quantitative performance comparison in terms of PSNR measurements (Table 2).

Filtering of images corrupted by Noise Model 2: Experiments were carried out on corrupted (80% noise density) 'Lena', 'Tire' and 'Cameraman' images, where each of the image was corrupted with different densities (probabilities of occurrences) of 'pepper' (i.e., 0) and 'salt' (i.e., 255), based on Noise Model 2. The performance results are shown in Table 3. It may be observed that the proposed algorithm still works quite well for unequal densities of 'salt' and 'pepper' noise, provided that neither the density of 'salt' nor that of 'pepper' is equal to or more than 50%. This is due to the fact

Fig. 9 Results of denoising corrupted images "Lena," "Cameraman," and "Tire" (with 50% impulse noise density (30% salt and 20% pepper), the range of noise are [0; 19] and [236; 255]) by using proposed directional switching median filter (*first column*), the existing switching median filter with the BDND incorporated (*second column*), respectively

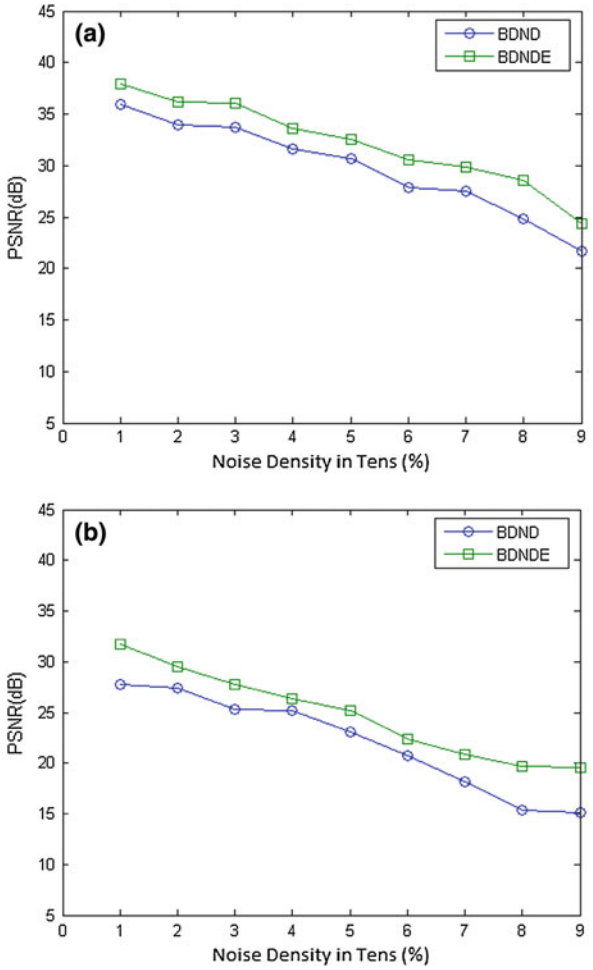

Fig. 10 PSNR performance comparison of using the BDND, the proposed directional switching median filter on: **a** "Cameraman;" and **b** "Lena;" corrupted by various noise densities (model 4)

that the proposed method depends on the median of the windowed pixels as the first key step, and the computed median is quite likely a noise in these cases. The visual results are shown in Fig. 5. Figure 6 graphically illustrates the quantitative performance comparison in terms of PSNR measurements.

Filtering of images corrupted by Noise Model 3: Several experiments were carried out for noise model 3, with various corruptions ranges of both low intensity and high intensity. Table 4 outlines the results for test images 'Lena', 'Tire' and 'Cameraman'. Figure 7 demonstrated the resultant images for gray scale images, and Fig. 8 graphically illustrates the quantitative performance comparison in terms of PSNR measurements. In our experiments, the value of m was taken as 20 for the performance analysis.

Filtering of images corrupted by Noise Model 4: From Table 5, it is evident that the proposed algorithm works fairly well under this model, provided that neither of the noise density $\geq$50%. This is due to the same reason as explained in the Noise Model 2. Table 5 shows the results for test images 'Lena', 'Tire' and 'Cameraman'. Figure 9 demonstrated the resultant images for gray scale images and Fig. 10 graphically illustrates the quantitative performance. The value of m was taken as 20 for the performance analysis.

It may be observed from the results that for high corruption level, our proposed method performs better compared to that of the BDND filter. It also gives higher PSNR value and better image quality than that of the BDND. Since the noise detection plays the key role on denoising, it would be insightful to evaluate the performance purely contributed from that part, in terms of the number of miss detection (MD) (impulse noise being miss detected) and that of false alarm (FA) (uncorrupted pixel being misclassified as noise). The new detection algorithm can reduce the miss-detection and false-alarm rate significantly even in random noise densities. As noise increases, the BDND results in a high false alarm while the proposed algorithm can reduce this value, and this account for large performance gain. Also, the execution time (ET) of

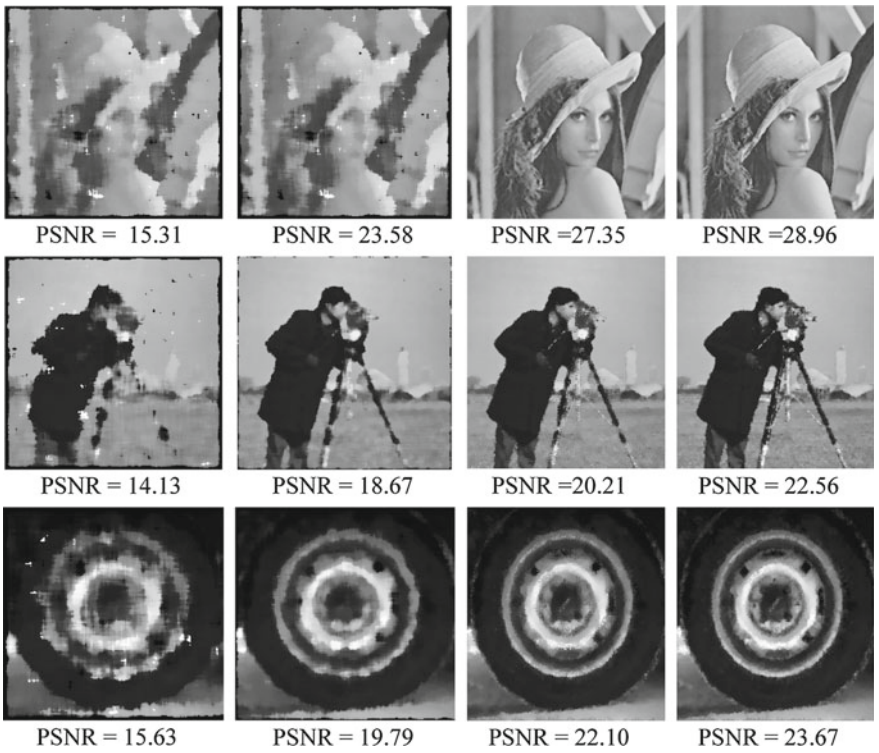

Fig. 11 Results of denoising corrupted images "Lena," "Cameraman," and "Tire" (80% impulse noise density (model 1)) by using **a** SMF using window size 13 × 13 **b** DWMF **c** BDND filter and **d** proposed BDNDE filter, respectively

the algorithm is significantly less compared to BDND. The execution can be further enhanced (in the case of salt-and-pepper noise) by applying only one iteration (21 × 21 only and 2 iteration should be needed for random noise) in the proposed detection phase, so that it can gain better result in miss-detection and false-alarm rate.

The performance of the proposed method has also been compared with conventional filter such as standard median filter (SMF) and advanced filter such as directional weighted median filter (DWMF) [18]. The visual results of the filtered images are shown in Fig. 11 for comparative analysis. From the visual results, it is evident that the proposed method gives better output and better edge detail preservation compared to other filters. Therefore, through quantitative analysis, it was proved that our proposed BDNDE method gives higher PSNR values compared to other filters.

The result of gray scale image restoration clearly demonstrates that the proposed method produces better results compared to the BDND-based filtering. We therefore advocate that the application of directional filtering process conditionally across the filtering window in our proposed new method significantly preserves edge details ensuring that the resulting image has better clarity, compared to the images obtained using other methods.

5 Conclusion

In this paper, we proposed a novel, accurate and simple-to-implement impulse-noise detection method, which utilizes an enhanced switching median filter. Additional improvements were also made in the noise-adaptive filtering stage as described in Sect. 3.2. To evaluate the performance variations often encountered in practical cases, four noise models were used to generate impulse noise. Extensive simulation results demonstrated that our filter consistently shows better results compared to BDND filtering (especially, with a large margin of improvement at extremely high noise density corruption) by attaining much higher PSNR across a wide range of noise densities (from 10 to 90%). The key success of such performance delivery is mainly due to highly accurate noise detection, achieving zero miss-detection rate (very low for random noise) up to 90% noise density corruption (based on Noise Model 1), while maintaining a fairly low false-alarm rate for other noise models. The proposed method improves filtering by applying a new directional filtering process conditionally across the filtering window, and this helps to preserve the edge details. This characteristic made the proposed image restoration technique simple, accurate and faster compared to the existing switching median filters. The new method has shown better performance in terms of subjective quality in the filtered image as well as objective quality in the peak signal-to-noise ratio (PSNR) measurement to that of the BDND filter.

Acknowledgments Authors sincerely acknowledge the management of (i) Rajagiri College of Social Sciences, Kalamassery, Kochi, India, (ii) Department of Computer Science, University of Kerala, Thriruvananthapuram, (iii) Naval Physical & Oceanographic Laboratory (NPOL), DRDO, Kochi, India and (iv) VIT University, Vellore, Tamil Nadu, India, for their unstinting support and infrastructural facilities provided.

References

1. Bovik, A.: Handbook of Image and Video Processing. Academic, New York (2000)
2. Huang, T.S., Yang, G.J., Tang, G.Y.: Fast two-dimensional medianfiltering algorithm. IEEE Trans. Acoustics Speech Signal Process **ASSP-1**(1), 13–18 (1979)
3. Pitas, I., Venetsanopoulos, A.N.: Order statistics in digital image processing. Proc. IEEE **80**(12), 1893–1921 (1992)
4. Brownrigg, D.R.K.: The weighted median filter. Commun. ACM **27**(8), 807–818 (1984)
5. Ko, S.-J., Lee, Y.H.: Center weighted median filters and their applications to image enhancement. IEEE Trans. Circuits Syst. **38**(9), 984–993 (1991)
6. Nair, M.S., Revathy, K., Tatavarti, R.: An improved Decision-based algorithm for impulse noise removal In: Proceedings of 2008 International Congress on Image and Signal Processing—CISP 2008, vol. 1, pp. 426–431. IEEE Computer Society Press, Sanya, Hainan, China, May (2008)
7. Nair, M.S., Revathy, K., Tatavarti, R.: Removal of Salt-and-Pepper noise in images: a new decision-based Algorithm. In: Proceedings of IAENG International Conference on Imaging Engineering—ICIE 2008, vol. 1, pp.611–616. IAENG International Multiconference of Engineers and Computer Scientists—IMECS 2008, Hong Kong, March (2008)
8. Sun, T., Neuvo, Y.: Detail-preserving median based filters in image processing. Pattern Recognit. Lett. **15**(4), 341–347 (1994)
9. Florencio, D.A., Schafer, R.W.: Decision-based median filter using local signal statistics. In: Proceedings SPIE Vis. Commun. Image Process., vol. 2308, pp. 268–275, Sep (1994)
10. Chen, T., Ma, K.-K., Chen, L.-H.: Tri-state median filter for image denoising. IEEE Trans. Image Process. **8**(12), 1834–1838 (1999)
11. Wang, Z., Zhang, D.: Progressive switching median filter for the removal of impulse noise from highly corrupted images. IEEE Trans. Circuits Syst. II **46**(1), 78–80 (1999)
12. Zhang, S., Karim, M.A.: A new impulse detector for switching median filters. IEEE Signal Process. Lett. **9**(4), 360–363 (2002)
13. Eng, H.-L., Ma, K.-K.: Noise adaptive soft-switching median filter. IEEE Trans. Image Process **10**(2), 242–251 (2001)
14. Pok, G., Liu, J.-C., Nair, A.S.: Selective removal of impulse noise based on homogeneity level information. IEEE Trans. Image Process **12**(1), 85–92 (2003)
15. Hwang, H., Haddad, R.A.: Adaptive median filters: new algorithms and results. IEEE Trans. Image Process. **4**(4), 499–502 (1995)
16. Ng, P.-E., Ma, K.-K.: A switching median filter with boundary discriminative noise detection for extremely corrupted images. IEEE Trans. Image Process. **15**(6), 1506–1516 (2006)
17. Ping, W., Junli, L,, Dongming, L., Gang, C.: A fast and reliable switching median filter for highly corrupted images by impulse noise. In: IEEE International Symposium on Circuits and Systems, ISCAS, pp. 3427–3430, June 2007 (2007)
18. Dong, Y., Xu, S.: A new directional weighted median filter for removal of random-valued impulse noise. IEEE Signal Process. Lett. **14**(3), 193–196 (2007)